

Saturated Absorption with Spatially Separated Laser Fields: Observation of Optical "Ramsey" Fringes*

J. C. Bergquist, S. A. Lee, and J. L. Hall†

*Joint Institute for Laboratory Astrophysics, National Bureau of Standards and University of Colorado,
Boulder, Colorado 80309
(Received 6 December 1976)*

We have observed Ramsey's interference fringes in the optical region using saturated-absorption techniques in a fast atomic beam. We discuss their physical origin and describe an optical configuration that guarantees fringes of high symmetry. This technique, with its high-resolution potential, should lead to dramatic improvements in spectral measurements.

In high-resolution optical spectroscopy, Doppler broadening and transit-time broadening pose problems. Doppler broadening can be nearly eliminated by two nonlinear techniques—saturated absorption and two-photon spectroscopy. Transit-time broadening due to the absorber's motion through the light beam can be reduced by using larger apertures. For example with a 30-cm aperture, resolution of $\sim 10^{11}$ was recently obtained.¹ Further scaling to approach the 10^{12} – 10^{13} resolution domain is troublesome, since large aberration-free wavefronts would be needed. In the microwave region, one of the most successful techniques for obtaining high resolution is Ramsey's method of using the interference arising from the interaction of a quantum absorber with two separated regions of the radiation field.² Synthesis of this "Ramsey" idea with nonlinear spectroscopy has been studied.³⁻⁷ In the case of two-photon spectroscopy, it is sufficient to use two Doppler-free interactions separated in time, and this type of optical Ramsey effect has recently been observed by Salour.⁸ In saturated absorption, both the Doppler effect and the shortness of the wavelength need to be considered. As we discuss later, to obtain high resolution with "Ramsey" interference, we need three separated radiation zones.⁹ The periodic phase shift between corresponding points on adjacent "Ramsey" fringes will be developed by a smaller frequency interval if the interzone transit time is increased.

We now describe the first experimental observation of three-zone optical "Ramsey" fringes. The experiment, shown in Fig. 1, used a monovelocity beam¹⁰ of metastable neon atoms interacting with spatially separated light beams from a frequency-stabilized single-mode dye laser. A few microamperes of $^{20}\text{Ne}^+$ from a hot-cathode ion source were accelerated to 5–50 keV and focused through a Na oven. Efficient charge exchange occurred via the reaction $\text{Ne}^+ + \text{Na} \rightarrow \text{Ne}(1s_5)$

+ Na^+ with an energy defect of only ~ 0.2 eV. The metastable-atom beam was about 2 mm in diameter and in the 2-mrad forward cone, the spread in velocities was $\Delta v/v \lesssim 10^{-4}$.

Saturation of the $1s_5 \rightarrow 2p_2$ (5882-Å) transition was adequate at 50-mW laser power even for our fast atom beam ($v/c \sim 10^{-3}$). The interaction was detected with high sensitivity via the strong $2p_2 \rightarrow 1s_2$ fluorescence (6599 Å) with an appropriately filtered photomultiplier. The ^{20}Ne atomic system, being free of hyperfine structure, facilitates a clear interpretation of our results.

The fringes are produced by the transport of phase information between the separated radiation zones by the atom's induced dipole polarization. In our experiment the spatial separation of adjacent radiation zones was $\sim \frac{1}{2}$ cm. At a typical beam energy (≈ 20 keV), the upper-state lifetime¹¹ (18.7 ± 0.3 nsec) gives a population decay length of 0.8 cm and a corresponding phase coherence

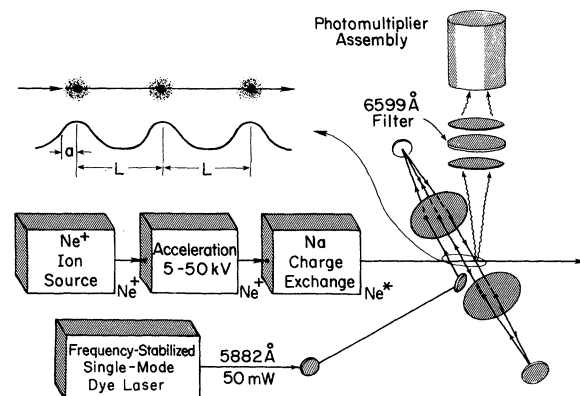


FIG. 1. Schematic of experiment. The three standing-wave interaction regions are formed by two well-corrected cat's-eye retroreflectors. Typical values are the following: $i(\text{Ne}^+) = 3 \mu\text{A}$, $V = 20$ kV, and the laser power is 50 mW. Fluorescence signal $\sim 10^8$ photons/sec reach the multiplier through the $f/2$ collection optics and filter.

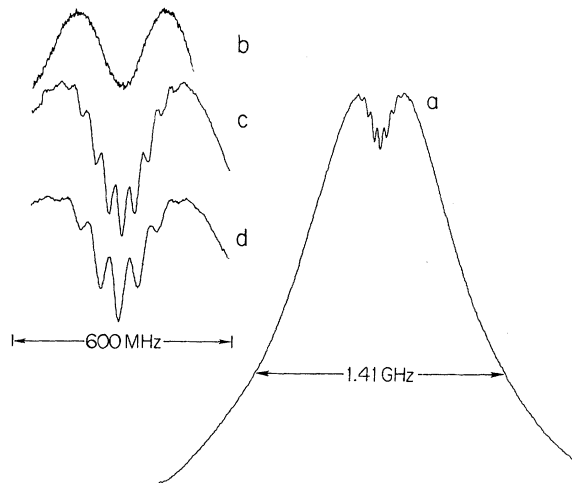


FIG. 2. Fluorescence signals. Curve *a*, most of beam Doppler profile (full width at half-maximum of 1.41 GHz) showing saturation dip and Ramsey fringes; $V = 19.5$ kV. Fringe contrast $\approx 3.8\%$. Curve *b*, saturation dip observed with two separated laser beams, $V = 19.5$ kV. Curves *c* and *d*, Ramsey fringes and saturation dips at $V = 35$ kV. Curve *c*, three beams; and curve *d*, four beams.

or “dipole” decay length of 1.6 cm. Symmetric fringes result when the spatial phases in the three zones are such that they appear to be samples of a large planar wave front. A simple yet elegant optical system that intrinsically provides this condition is formed by the opposition of two cat’s-eye retroreflectors. Fermat’s principle, applied to the optical system depicted in Fig. 1, shows that the necessary constant-phase condition is indeed satisfied.

The experimental observations are shown in Fig. 2. Figure 2(a) shows most of the beam Doppler profile, the saturated absorption dip, and the fringes due to the interaction with three equally spaced standing-wave radiation zones. In the inset, we compare the signals of three different beam geometries. The upper trace [Fig. 2(b)] is the fluorescence profile produced when the atomic beam intercepts only two standing waves. No fringes due to the interaction with two separated laser beams are observed on the saturated-absorption dip. The middle trace [Fig. 2(c)] shows the profile for three equally spaced standing waves—one easily observes the optical “Ramsey” fringes. Their expected form⁷ is a cosine function multiplied by the saturated-absorption envelope.

In Fig. 3(a) we pictorially represent the lowest-order terms of an atom’s radiative interaction

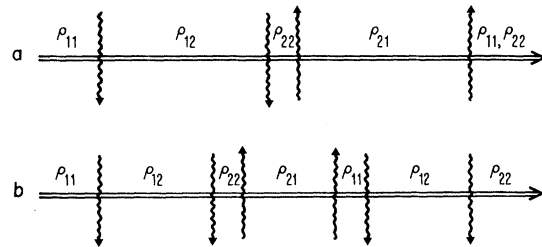


FIG. 3. Diagrammatic representation of the origin of Ramsey fringes in saturation spectroscopy. Double arrows represent atom beam. Laser beams are represented by wavy arrows. (a) Three-zone case; contribution by the other diagram in the standing-wave case is coherent. (b) One term in the four-zone case.

with three zones. The atoms of interest interact to first order with one running component (say, the + one) in the first light zone (at $x = 0$) to produce a polarization ρ_{12} which is carried with its natural precession and decay into the second illuminated zone (at $x = L$). Here a second interaction, with the (+)-running component, produces a velocity-resolved upper-state population ρ_{22} . The excited atoms now interact with the (-)-running component to produce a polarization ρ_{21} . This polarization carries with it geometrical phase information which will be discussed below. In the third zone (at $x = 2L$) our atoms interact with a (-) component to produce a ground-state population ρ_{11} , and the detected excited-state population ρ_{22} . This sequence of four interactions¹² produces in the upper- and lower-state populations a change which is nonlinear in the laser intensity and which manifests the Ramsey interference structure as a function of detuning.¹³ It is expected that at higher laser field strengths one would see optical nutation and oscillation with intensity of the fringe amplitudes.

The geometrical aspects of this interaction sequence deserve comment.¹⁴ Since the interaction regions are large compared with a wavelength, the density matrix elements discussed above contain rapidly varying geometrical phase factors. One can show that if the third zone is located at $x = 2L$, the phases associated with both the entry position and the Doppler velocity vanish. One also finds the fringe phase due to detuning has a periodicity of π . We further note that the observed fringe signals arise from an angular slice of the atom beam $\delta\theta \sim \lambda/3a$, defined by the transit-limited saturation in one zone. By contrast, if the radiation field filled the entire effective aperture of $2L$, only particles in the much smaller angular

interval $\delta\theta' \sim \lambda/3L$ could contribute.

The fringes produced with four equally spaced light zones are shown in Fig. 2(d). In this case the spacing between adjacent zones was 3 mm, about $\frac{2}{3}$ that of the three-beam case. Thus the fringe frequency separation is about $\frac{3}{2}$ times the previous value. Figure 3(b) gives pictorial representation of one term in the four-beam case. There are many possible diagrams at high intensity or with several beams.

With three beams, the frequency separation of the m th fringe from the central one, $\Delta\nu_m$, was measured as a function of the atom beam velocity. The expected relation $\Delta\nu_m = \frac{1}{2}m(v/L)$, with $m = \pm 1, \pm 2, \pm 3$, was found to be satisfied to within the experimental precision of $\lesssim 10\%$.

The shape of the fringes is symmetric due to the intrinsic equal-time property of the cat's-eye retroreflectors, if they have ideal lenses and are correctly focused.¹⁵ If the cat's eye containing three beams is slightly defocused, one shifts the phase of the outer zones with respect to the inner zone, and thus the fringe shape contains an admixture of absorption and dispersion. Under suitable conditions we obtained a line shape which had dispersion-shaped fringes but which was flat near zero detuning. To recover the fringes alone, one could phase-modulate one of the zones, for example with matched, opposite-polarity, electro-optic crystals.

An important advantage of Ramsey's method is that most of the atomic phase evolves when the atoms are not interacting with the radiation field. In saturation spectroscopy, power broadening will thus be minimized. (We easily observed linewidths as narrow as the 4.3-MHz natural half-width.) In two-photon spectroscopy, this field-free evolution results in a smaller net ac Stark effect of the line center, as was noted by Baklanov, Chebotayev, and Dubetskii.⁶ Furthermore, the two-photon transition probability per unit Stark shift can be enhanced by focusing. Extremely high resolutions may be expected for atoms such as bismuth and silver which possess two-photon-accessible metastable levels.¹⁶

In conclusion, we have observed optical "Ramsey" fringes with the technique of spatially separated beams. We have shown that their symmetry is very good with an interferometric quality cat's-eye retroreflector, and so it will be possible to frequency-lock to them with high precision. For example, this technique may afford an important improvement in the measurement of the relativistic Doppler shift.¹⁰ The possibility of ap-

plying this scheme to the calcium $^1S_0 - ^3P_1$ (6573-Å) transition¹⁷ with its 400-Hz natural-linewidth limit is tantalizing.¹⁸ We suggested phase-modulating one zone to allow clean recovery of the fringe information. Finally, with the high-intensity theory¹⁹ (program SHAPE), we have synthesized the optical fringes for separated Gaussian beams, and for three-zone annular apertures. These aperture-induced fringes have been observed by one of us (J.C.B.) in an external CH_4 cell at 3.39 μm .

The authors are grateful to C. J. Bordé for stimulating discussions about the theory of these effects.

*This work has been supported in part by the National Science Foundation under grant No. PHY76-04761 and by the National Bureau of Standards as part of its research programs on improved precision measurement for application to basic standards.

[†]Staff Member, Laboratory Astrophysics Division, U. S. National Bureau of Standards.

¹J. L. Hall, C. J. Bordé, and K. Uehara, *Phys. Rev. Lett.* **37**, 1339 (1976).

²N. F. Ramsey, *Phys. Rev.* **78**, 695 (1950).

³V. S. Letokhov and B. D. Pavlik, *Opt. Spectrosc. (U.S.S.R.)* **32**, 455 (1972).

⁴J. L. Hall, in *Atomic Physics 3*, edited by S. J. Smith and G. K. Walters (Plenum, New York, 1973), pp. 615-646.

⁵Ye. V. Baklanov, B. Ya. Dubetskii, and V. P. Chebotayev, *Appl. Phys.* **9**, 171 (1976); B. Ya. Dubetskii, *Sov. J. Quantum Electron.* **6**, 682 (1976).

⁶Ye. V. Baklanov, V. P. Chebotayev, and B. Ya. Dubetskii, *Appl. Phys.* **11**, 201 (1976).

⁷C. J. Bordé, private communication, and to be published.

⁸M. Salour, *Bull. Am. Phys. Soc.* **21**, 1245 (1976).

⁹In Ref. 4, the "Ramsey" fringes were observable only because the two beams were so close together.

¹⁰J. J. Snyder and J. L. Hall, in *Lecture Notes in Physics*, edited by S. Haroche, J. C. Pebay-Peyroula, T. W. Hänsch, and S. E. Harris (Springer, Berlin, 1975), Vol. 43, pp. 6-17.

¹¹D. Frölich, J. J. Snyder, and J. L. Hall, to be published. Also see W. R. Bennett, Jr. and P. J. Kindlman, *Phys. Rev.* **149**, 38 (1966).

¹²We observed fringes with a standing wave in zone two and counter-running waves in zones one and three, but three standing waves were more convenient experimentally.

¹³We expected and confirmed experimentally that fringe contrast could be enhanced by monitoring the fluorescence only from the third zone and beyond.

¹⁴The standing-wave case was studied in Ref. 5.

¹⁵J. J. Snyder, *Appl. Opt.* **14**, 1825 (1975).

¹⁶P. L. Bender, J. L. Hall, R. H. Garstang, F. M. J. Pichanick, W. W. Smith, R. L. Barger, and J. B. West, *Bull. Am. Phys. Soc.* **21**, 599 (1976).

¹⁷R. L. Barger, T. C. English, and J. B. West, Opt. Commun. **18**, 58 (1976).

¹⁸Especially if we consider widely separated beams

to select "aged" atoms.

¹⁹C. J. Bordé, J. L. Hall, and C. V. Kunasz, to be published.

Nonlinear Evolution of Runaway-Electron Distribution and Time-Dependent Synchrotron Emission from Tokamaks*

C. S. Liu and Y. Mok

Department of Physics and Astronomy, University of Maryland, College Park, Maryland 20742
(Received 20 May 1976)

Stability of the runaway electrons in tokamaks is analyzed. The distinction between high-density and low-density operation of tokamak discharges is interpreted in terms of the stability condition obtained. In the unstable case, the temporal evolution of the distribution function of the runaway electrons is obtained by solving the quasilinear equation. Time-dependent synchrotron emission from the runaway electrons is calculated.

Recent measurements of cyclotron radiation from low-density tokamak plasmas have shown significantly nonthermal properties¹⁻³: The radiation intensity is more than an order of magnitude above the thermal level expected from the measured temperature, with a broad frequency spectrum having minima at the gyroharmonics⁴; the radiation level is nonsteady with sudden ($\leq 10 \mu\text{sec}$) increases in intensity, correlated with loop-voltage spikes,⁴ with bursts of x rays and of radiation from ω_{pe} to ω_{pi} , and with the ion heating.⁵ In this Letter, we attempt to interpret this enhanced radiation as synchrotron emission by the runaway electrons.⁶

A specific distribution function of the runaway electrons is obtained by solving the Fokker-Planck equation in the steady state, and this distribution is then used as the unperturbed runaway distribution for stability analysis. In the unstable region, the time-dependent quasilinear equation is solved analytically to obtain the nonlinear evolution of the runaway distribution. With this time-dependent distribution function of the runaway electrons, we calculate the time evolution of the spectrum of their synchrotron emission, including the effect of reabsorption by the background plasma.

We solve the Fokker-Planck equation in the runaway region where $v_{\parallel} > v_c = (E_0/E)^{1/2}v_e$, $v_e = (2T_e/m)^{1/2}$, $E_0 = e \ln \Lambda / \lambda_D^2$, and $\lambda_D^2 = T_e / 4\pi n e^2$. Included is a loss term of the form $-v_{\parallel} f / v_L \tau_0$, as a model to account for the loss of high-energy electrons caused by the imperfect magnetic surfaces,⁷ where τ_0^{-1} is the loss rate of particles with $v_{\parallel} > v_L$. To have a steady state, a source at low energy is introduced to maintain a constant rate, γ_0 , of runaway production given by⁸ $\gamma_0 = 0.35\nu_0(E/E_0)^{-3/8} \exp\{-[(2E_0/E)^{1/2} + E_0/4E]\}$, where ν_0 is the electron-electron collision frequency. The Fokker-Planck equation in the runaway region⁸ is then solved for $v_{\parallel} \gg v_c$ to obtain the following steady-state solution

$$f_R = 2\Delta n \frac{E}{E_0} \left[\pi^{3/2} v_e^2 v_0 \ln \left(\frac{E}{E_0} \frac{v_{\parallel}^2}{v_e^2} \right) \right]^{-1} \exp \left\{ \frac{E}{E_0} v_{\perp}^2 \left[v_e^2 \ln \left(\frac{E}{E_0} \frac{v_{\parallel}^2}{v_e^2} \right) \right]^{-1} + \frac{v_{\parallel}^2}{v_0^2} \right\}. \quad (1)$$

The normalization is so chosen that the loss of the runaways is balanced by the runaway production, i.e., $\Delta n / \tau = n_0 \gamma_0$, where $\Delta n / n_0$ is the density ratio of the runaways to the bulk thermal electrons, and τ is the average life time of runaway electrons. Moreover, v_{\perp} and v_{\parallel} are the velocity components perpendicular and parallel to the electric field, and $v_0 = [E\nu_0\tau_0/E_0]^{1/2}v_L$ is the effective cutoff velocity. Typically, for low-density discharges, the observed energy of the runaways is cut off at about 200 keV, corresponding to a value of $v_0/v_e \approx 12$ for a bulk electron temperature of 0.7 keV. Note that the effective perpendicular temperature of the runaways is enhanced by a factor $(E_0/E) \ln[E v_{\parallel}^2 / E_0 v_e^2]$ with the logarithmic factor typically about 2, and is an order of magnitude less than the parallel temperature.

For the stability analysis, we choose, for simplicity, the unperturbed distribution to be a composite of a bulk of Maxwellian electrons $v_{\parallel} \leq v_c = v_e(E_0/E)^{1/2}$ and a runaway tail given by Eq. (1) for $v_{\parallel} > v_c$ in a magnetic field aligned with the inductive electric field. The anisotropy of the runaway distribution can then drive the plasma wave unstable through the anomalous cyclotron resonance $\omega_k + \Omega = k_{\parallel} v_{\parallel}$.⁹ This instability was first qualitatively examined by Kadomtsev and Pogutse and its quasilinear effects have been qualitatively studied by Shapiro and Shevchenko.⁹ Here we use the explicit runaway distribution given by (1) to obtain a definite stability boundary and the quasilinear evolution of the distribution need-